Cationic local composition fluctuations in rapidly cooled nuclear fuel melts

Mohamed Jizzini, Emmanuelle Brackx, Pascal Piluso, Denis Menut, René Guinebretière

▶ **To cite this version:**

Mohamed Jizzini, Emmanuelle Brackx, Pascal Piluso, Denis Menut, René Guinebretière. Cationic local composition fluctuations in rapidly cooled nuclear fuel melts. Nuclear Materials and Energy, 31 (14), pp.101183, 2022, 10.1016/j.nme.2022.101183 . cea-04721890

HAL Id: cea-04721890
https://cea.hal.science/cea-04721890v1

Submitted on 13 Nov 2024

HAL is a multi-disciplinary open access archive for the deposit and dissemination of scientific research documents, whether they are published or not. The documents may come from teaching and research institutions in France or abroad, or from public or private research centers.

L'archive ouverte pluridisciplinaire **HAL**, est destinée au dépôt et à la diffusion de documents scientifiques de niveau recherche, publiés ou non, émanant des établissements d'enseignement et de recherche français ou étrangers, des laboratoires publics ou privés.

Distributed under a Creative Commons Attribution - NonCommercial 4.0 International License

Version of Record: https://www.sciencedirect.com/science/article/pii/S2352179122000680
Manuscript_1c68615820e96eeebc5f57ce9acf4977

Cationic local composition fluctuations in rapidly cooled nuclear fuel melts

Mohamed Jizzini[a,b], Emmanuelle Brackx[a], Pascal Piluso[c], Denis Menut[d], René Guinebretière[b,*]

[a]*CEA, DES, ISEC, DMRC, SASP, LMAT, Univ Montpellier, Marcoule, France;*

[b]*Université de Limoges, IRCER, UMR CRNS 7315, France;*

[c]*CEA/DES/IRESNE/DTN/SMTA, LEAG, Cadarache, France;* [d] *SOLEIL Synchrotron, MARS beamline, France*

* Corresponding author. René Guinebretière, IRCER, UMR CNRS 7315, 12 rue Atlantis, Limoges, 87068, France. E-mail address: rene.guinebretiere@unilim.fr

During a severe accident in a nuclear reactor, as it occurred in Fukushima Daiichi BWRs in 2011, the so-called “corium” resulting from the thermal fusion of nuclear fuel and interaction with the zircaloy cladding at high temperature (T>2800 K) can be formed. During cooling phases in the vessel or outside of the vessel, corium is crystallized at solid state under the form of an uranium and zirconium oxide solid solution. Based on the severe accident scenario, different phenomena can occur such as Fuel Coolant Interaction (FCI). In those conditions, solidification paths will be far from thermodynamic equilibrium if the corium is cooled very quickly by interacting with water. At the CEA-Cadarache, on the PLINIUS Severe Accident Platform, FCI is studied at the KROTOS experimental facility using prototypical corium, *i.e.* with depleted uranium dioxide. Resulting from different stages of corium - water interaction, we hypothesis that a large cationic composition fluctuation takes place into these $U_{1-x}Zr_xO_{2\pm y}$ crystals. Thanks to high-resolution X-ray diffraction experiments done at the SOLEIL synchrotron radiation source at the MARS beamline, we were able to analyze at the quantitative level the cationic composition fluctuations that are strongly related to the cooling speed.

© 2022 published by Elsevier. This manuscript is made available under the CC BY NC user license
https://creativecommons.org/licenses/by-nc/4.0/

Keywords: corium, cationic composition fluctuation, X-ray diffraction

1. Introduction

In case of a severe accident in a nuclear reactor, as it happened in Fukushima Daiichi, a complex mixture, so-called corium, is formed at very high temperature (T > 2800 K) under various conditions of oxygen potential [1]. This hot fluid is initially mainly composed of nuclear fuel (UO_2) and oxidized zirconium coming from the zircaloy cladding operated in Light Water Reactors (LWR). The downward relocation of this corium into the remaining core water, or injection of fresh water promotes several scenarios of hot fluid cooling and consequently different paths of the solidification [2]. This key phenomenon for nuclear safety is experimentally studied at the KROTOS facility. S.B. Board and R.E. Hall [3] have proposed four main steps to describe FCI and its possible consequence, *i.e.* Steam Explosion (SE). This kind of configuration is simulated on KROTOS facility with a corium jet at about 2800 K poured into cold water (see Fig. 1):

(1) *Premixing* – The corium jet is fragmented in the coolant by hydrodynamic forces into coarse droplets covered by a steam film limiting heat transfer and solidification occurs in few seconds

(2) *Triggering* - The protective steam film can locally be destabilized. In this case, in a few milliseconds, the

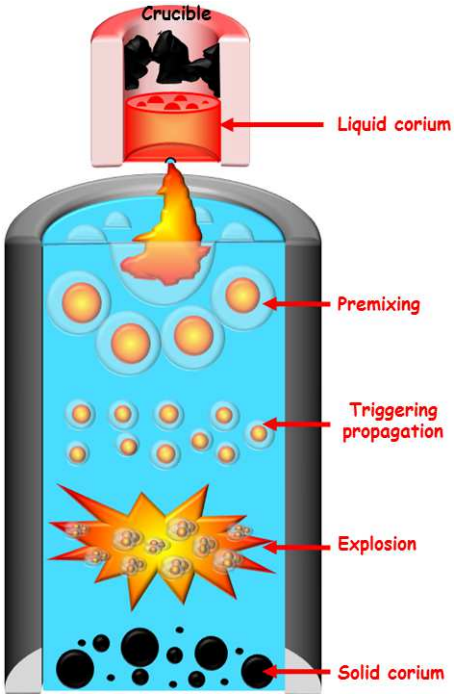

Fig. 1. Schematic representation of the KROTOS facility at CEA-Cadarache. The FCI is involving four different phenomena that take place according to very different time scales.

melt is locally divided into fine droplets by thermal fragmentation

(3) *Propagation* – In few tens of milliseconds, thermal fragmentation process escalates through the premixed volume. The propagation wave can reach supersonic velocities

(4) *Expansion (steam explosion*) – in few microseconds, the thermal energy of the melt is finally transferred to water, forming steam in a very short time scale and generating consequently high-pressure loads on the reactor vessel (in-vessel configuration) or reactor pit (ex-vessel configuration).

The solidification path of the corium from liquid state to solid state is out of thermal and thermodynamic equilibrium [4]. Nevertheless, the knowledge of the final solid state of corium is a key issue for the understanding, modelling and mitigation of severe accident phenomena and for future activities in damaged reactors decommissioning. In order to decouple the phenomena, studies have been focused on ternary corium compositions $U_{1-x}Zr_xO_{2\pm y}$ [5]. We think in this work that this corium solid solution exhibits a very large cationic composition fluctuation that we were able to analyze at the quantitative level through high-resolution x-ray diffraction (HR-XRD) measurements. Moreover, we find that the shape of the determined cationic distributions is strongly linked to the cooling process.

2. Materials and methods

Samples studied in the present paper are coming from the KROTOS "KA2" test realized in the frame of the French ANR-ICE program. The initial composition with respect to the raw materials was 80.1 wt.% UO_2; 11.4 wt% ZrO_2; 8.5 wt% Zr, that corresponds to an atomic ratio between oxygen and cations equal to 1.61, representative of LWR operating conditions. The raw materials were mixed and melted at 3040 K with

superheat of about 200 K according to the theoretical liquidus temperature of the mixture in the upper crucible of the facility [6]. After the release of the corium with its crucible on a puncher with a tin membrane, the liquid corium was poured into the KROTOS test section, full of water at liquid state maintained at 333 K under a pressure of 2 bars. During cooling, the corium is interacting with water and therefore the final oxygen stoichiometry of the corium solid phase is indeed unknown.

Post-test analyses have been performed on three corium sample families, representative of specific cooling regimes. The samples are as follows: (i) The KA2-crucible, representative of a "slow cooling rate" of corium located in the crucible after the test. Cooled naturally under argon in a few minutes, this sample didn't interact with water and presents solidification of melt in inert atmosphere. (ii) The KA2-200, representative of a "*fast cooling rate*", is made up of corium debris having a mean particle size close to 200 µm, formed after the interaction with water steam and cooled, mainly without explosion. (iii) The KA2-50, representative of a "*very fast cooling rate*", is made up of corium debris having a mean particle size of roughly 50 µm, formed after the interaction with water steam and cooled with explosion.

It has to be stressed that from the structural point of view, the final solid state of corium is due to several coupled non-linear and complex phenomena (oxidation, fragmentation, explosion, cooling and solidification) occurring far from the equilibrium. It is worth noting that at high temperature ZrO_2 adopts the $Fm\bar{3}m$ cubic space group that is observed for UO_2 at all temperatures. According to the pseudo-binary UO_2-ZrO_2 equilibrium phase diagram [6, 7], during cooling from the liquid state, the $U_{1-x}Zr_xO_2$ solid solution crystallizes under the $Fm\bar{3}m$ cubic space group whatever the value of x is. The tetragonal phase ($P4_2/nmc$ space group) has been found at room temperature under metastable state [8] only for compositions corresponding to x value above 0.7. As we

will show later in all the cases under consideration here, the value of *x* remains below 0.7 and the solid solution crystallizes under is cubic form.

Structural analyses of the corium samples were performed using the HR-XRD set-up CX2 at the MARS beamline at the synchrotron SOLEIL [9]. This beamline is fully devoted to the structural characterization of radioactive materials. The CX2 end-station is equipped with a four-circle diffractometer that we used in transmission mode. HR-XRD patterns were recorded using the Double Crystal Monochromator (DCM) equipped with a pair of Si (220) crystals which second crystal is bent for horizontal focusing. Before being collected by a set of 24 scintillation detectors, the X-ray beams diffracted by the samples are highly collimated using a multi-crystal analyzer stage [9] made of two banks of Ge (111) analyzer crystals mounted on the 2θ arms. Such multi-analyzer set-up was developed for beamlines using intermediate energy range around a number of synchrotron radiation sources [10, 11] and was recently extended to the case of beamline working at energies as high as 60 keV [12]. All the diffraction patterns considered in this article were obtained after the summation of the diffraction signals coming from all the 24 detectors. This summation was done using a specific procedure developed by the MARS beamline scientists. It is well-known that this geometry associated with a capillary sample holder is one of the most efficient ways to record very high-resolution diffraction patterns. Depending on the energy and the collimation of the beam the full width at half maximum (FWHM) of the diffraction peaks is lying typically between few thousandth and few hundredths of degree [11]. Taking into account the K-edge of zirconium, the energy of the beam was fixed at 17 keV after calibration using the absorption K-edge of a yttrium metallic foil. The size of the beam was about 300 x 1000 μm^2 (V x H). All the corium samples were milled and put into closed capillaries following a procedure proposed by Hill *et al.* [13] and already used

before on nuclear materials at the MARS beamline. The internal and external diameters of the capillaries were equal to 2 and 3 mm respectively. The total sample volume was close to 50 µL and in order to limit the X-ray beam absorption, the corium powders were diluted in wax (one third corium and two third wax). During the pattern recording, the samples were continuously rotated around the capillary axis. The instrumental resolution function was estimated through the diffraction pattern measurement of the LaB_6 660b NIST powder and the diffraction peak FWHM was close to 0.02 nm^{-1}, corresponding to 0.015°, according to the x-ray beam energy. Scanning electron microscopy (SEM) observations were realized using a Zeiss supra 55 electron microscope coupled with an electron back-scattered diffraction (EBSD) detector from the Bruker company.

3. Results and discussion

Part of the diffraction patterns recorded on the NIST standard powder and on the 3 different corium samples is reported in Fig. 2a. As evidenced by the enlargement around the (111) corium diffraction peak, both the profiles and the mean positions of these diffraction peaks are strongly influenced by the cooling process. In all cases, they exhibit a very significant asymmetric broadening with respect to the instrumental function (see in Fig. 2 the LaB_6 diffraction peak near the (111) corium peak). The broadening of the diffraction peaks can be related to a number of crystalline defects [14]. The three corium samples have been intensively characterized through SEM-EBSD analysis. It is worth noting that whatever the cooling process was, the size of the corium crystals is always much greater than one micron and often corresponds to a few tens of microns (see Fig. 2b). Thus, the X-ray diffraction peak broadening is not related to a crystal size effect.

As written above, the UO_2-ZrO_2 pseudo-binary phase diagram exhibits a large solid solution [6, 7] allowing a continuous variation of the cationic composition of the $U_{1-x}Zr_xO_2$ mixed oxide. Therefore, according to previous experiments done on similar compounds [8], the shape of the XRD peaks can be interpreted as a direct consequence

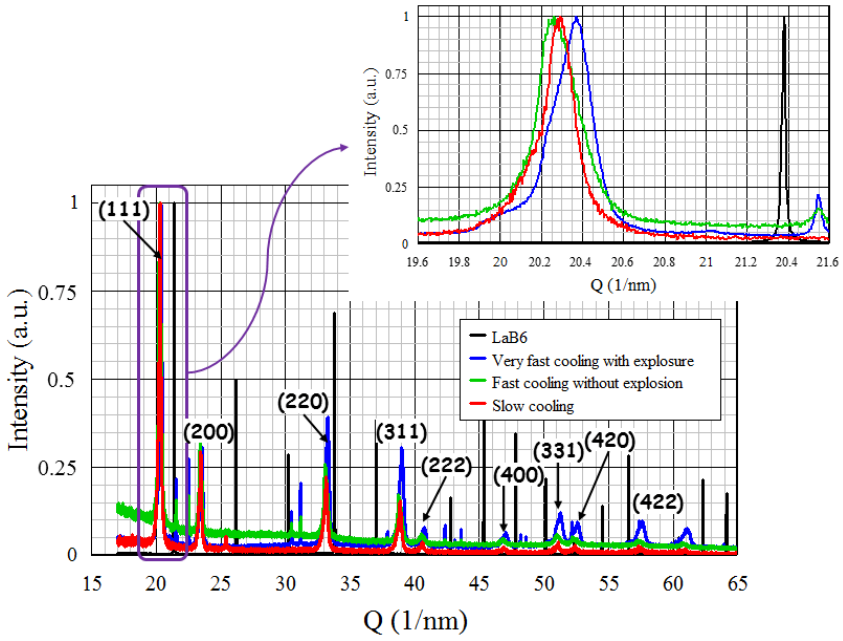

(a) XRD patterns recorded on the three corium samples and the LaB_6 660b NIST powder

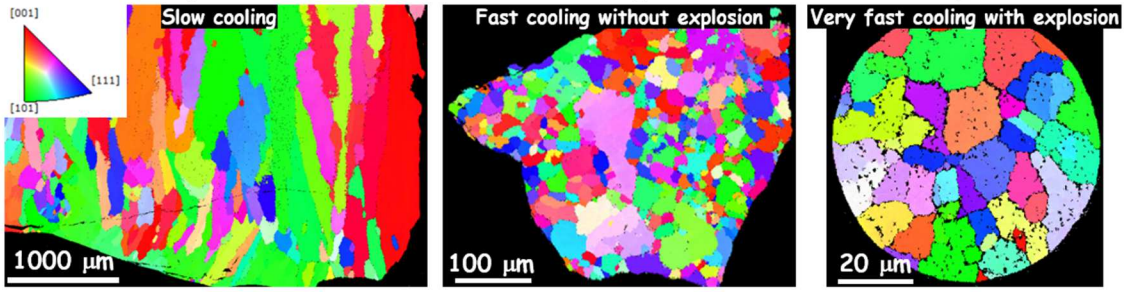

(b) SEM-EBSD image illustrating the typical size of the corium crystals. The color scale with respect to the crystal orientations is indicated on the left corner of the figure.

Fig. 2. Influence of the cooling process on the profile of the XRD diffraction peaks.

of local cationic composition fluctuations in each individual corium crystal. It is well-known that such local composition fluctuations in solid solutions may be associated to the presence of microstrains (see for example [15-17]). In principle, the line profile analysis of the diffraction peaks recorded on the polycrystalline samples may take into account simultaneously cationic fluctuation and microstrains. Although such a general

approach has been described for binary ordered or disordered metallic alloys [18], it is much more complex in the case of oxides. As a first step of the determination of the cationic local fluctuation in corium crystals, the potential associated microstrains will be neglected here.

In the frame of the X-ray diffraction kinematic theory, the experimental diffraction patterns can be considered as a summation of a number of patterns all indexed with respect to the $Fm\bar{3}m$ space group and corresponding to a local distribution of the cell parameter of this cubic $U_{1-x}Zr_xO_2$ solid solution. Knowing the relationship between the U/Zr atomic ratio and the value of this cell parameter, allows in principle to extract the cationic fluctuation from the cell parameter distribution. The basis of the quantitative analysis of diffraction pattern following this approach has been introduced in the seventies by C.R. Houska for the study of metallic alloys [19-22] and extended to the case of thin films [23, 24]. More recently, this approach was applied to ceramic-metal composite materials [25] and to the study of cationic local fluctuations in oxides [26]. The principles of the method are presented Fig. 3. It corresponds to the decomposition of each experimental peak profile into a set of *N elementary peaks* where each of them corresponds to a given cell parameter and thus to a given cationic composition. The profile of these elementary peaks was fixed as identical to the instrumental function at the corresponding Q-value. Due to their large broadening, the corium diffraction peaks are partially superimposed on each other and thus the experimental patterns were modelled by full pattern matching approach using the MAUD software [27]. All the diffraction peaks were simulated using the pseudo-Voigt function [28] and the Q evolution of the width of the instrumental function was fitted according to the Caglioti polynomial approximation [29]. Two inserts corresponding to zooms on both the low-Q and the high-Q parts of the diffraction pattern illustrate the

quality of the refinement. The values of the normalized difference function remains between -0.03 and 0.03 whatever the values of Q (see the bottom of Fig. 3, below the diffraction pattern). The values of the reliability factors obtained after the best fits are reported Table 1.

Table 1. Values of the reliability factors that attest of the quality of the fits.

	R_{WP} (%)	R_{exp}(%)	GofF
Slow cooling	5.265	9.02	0.584
Fast cooling without explosion	8.698	10.463	0.831
Very fast cooling with explosion	5.276	9.907	0.532

The narrow diffraction peaks observed on the pattern are corresponding to the diffraction by of tin crystals present as impurities in the sample. The contribution of this additional phase was considered during the full pattern matching process. The local composition fluctuations are extracted with respect to the variation of the corium cell parameter *a* as a function of zirconium amount *x* using the following linear equation: a=5.468-0.3296x [8, 30].

The three corium diffraction patterns were simulated according to this methodology introducing 50 patterns between UO_2 and ZrO_2 range, with a variation of 0.02 with respect to the value of "*x*". After refinement, 30 compositions between pure UO_2 and $U_{0.43}Zr_{0.57}O_{2.0}$ exhibiting a significant contribution have been identified. The

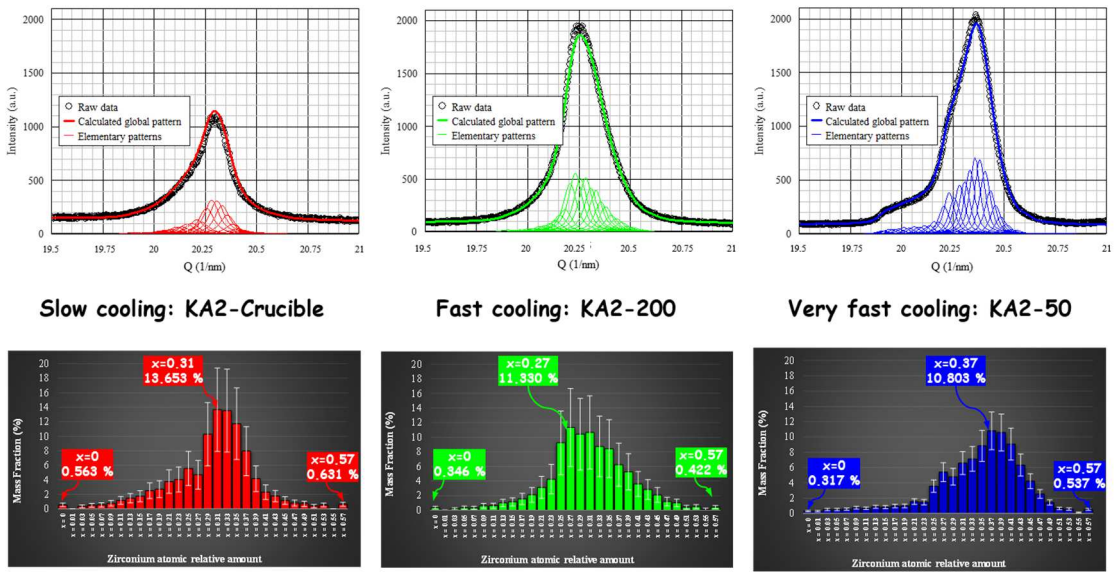

Fig. 4. Cationic composition fluctuations into corium crystals as a function of the cooling process.

cationic composition fluctuations obtained for each sample are reported Fig. 4 with an illustration of the diffraction patterns fitting with a focus on the enlargements around the (111) peak. The cationic distribution fluctuation is significantly influenced by the cooling process and the associated solidification path mechanism but also by oxidation mechanism. In relation with the corium cooling rate and the oxidation process, mechanisms can be proposed to explain the cationic fluctuation asymmetry curve evolution. In the crucible, conditions are the closest of the thermodynamic equilibrium, solidification process is slow, the curve can be considered as relatively symmetric and centered even if the spread is large. For fast cooling, the curve can be assumed as being "asymmetric" on the uranium rich side, whereas for very fast cooling, the curve can be assumed as being "asymmetric" on the zirconium rich side, both directly linked with the cooling rates.

4. Conclusion

FCI is a key phenomenon that can occur in case of a severe accident in a LWR. This phenomenon implies very quick process allowing high cooling rates and several solidification paths for the corium melt. Three prototypical corium samples coming from FCI experiments (KROTOS facility-CEA-Cadarache) have been studied through high-resolution x-ray diffraction experiments. The consequence of the different cooling rates is the formation of $U_{1-x}Zr_xO_2$ solid solutions crystallized under the $Fm\bar{3}m$ space group and exhibiting large and asymmetric cationic local fluctuations. It is worth noting that the formation of such continuous cationic composition fluctuations through spinodal process has been observed quite long time ago into yttrium doped zirconia [31, 32] that exhibit similar crystallographic structure of the samples under consideration here. Nevertheless, as far as we know, such HR-XRD experiments using synchrotron radiation and devoted to quantitative analysis of the cationic fluctuations have never

been done in corium. Moreover, their analysis at the quantitative level should be very helpful to better understand and model severe accident phenomena and to develop specific post-test analyses methodologies for use in decommissioning and storage operations of damaged Fukushima-Daiichi reactors. For a better understanding of corium behavior, the knowledge of solid state will be able to build a reliable modelling of severe accident phenomena, the final solid state acting as a signature of the severe accident phenomena. This first work has been able to show for the first time specificity of the cationic fluctuation in the corium solid solution $U_{1-x}Zr_xO_2$ using Large Instrument such as SOLEIL. Following this work, we will go on simulating more realistic corium solid state adding fission products immobilized in the corium such as strontium or barium. For the Fukushima Daiichi damaged reactors, it is planned to take some real corium samples and to perform post-test analyses before any decommissioning action. In the frame of OECD/NEA organization, international projects, such as *PreADES project* (“*Preparatory Study on Analysis of Fuel Debris”*), have been led to collect methodology on fuel debris characterization for Fukushima Daiichi damaged reactors and will go on in the next years.

Acknowledgements

The authors gratefully also thank the French research minister for the support to ICE-RSNR-post-Fukushima action (ANR-11-RSNR-0010).

References

[1] P. Piluso, B.R. Sehgal, K. Trambauer, B. Adroguer, F. Fichot, C. Muller, L. Meyer, W. Breitung, D. Magallon, C. Journeau, H. Alsmeyer, C. Housiadas, B. Clement, M.L. Ang, B. Chaumont, I. Ivanov, S. Marguet, J.P. Van Dorsselaere, J. Fleurot, P. Giordano, M. Cranga, Sarnet, Lecture Notes on Nuclear Reactor Severe Accident Phenomenology, CEA Cadarache, 2008.

[2] B.R. Sehgal. Appendix 1 - Corium Thermodynamics and Thermophysics. in Nucl. Saf. Light Water React., Academic Press, Boston. (2012) 657–673.

[3] S.J. Board, R.E. Hall. Third specialist meeting on sodium/fuel interaction in fast reactors, recent advances in understanding large-scale vapour explosion. Proc. Comm. Saf. Nucl. Install. (1975) 249–293.
[4] V. Tyrpekl, Effet matériaux lors de l'interaction corium-eau : analyse structurale des débris d'une explosion vapeur et mécanismes de solidification, PhD these, Strasbourg, 2012.
[5] P. Piluso, P. Fouquart, C. Brayer, V. Tyrpekl, C. Gueneau, T. Alpettaz, S. Grossé, The CEA Experimental Program Devoted to FCI Studies with Prototypical Corium, ERMSAR 15, Marseille, 2015.
[6] P.Y. Chevalier, E. Fischer, Thermodynamic modelling of the O–U–Zr system. J. Nucl. Mater. 257 (1998) 213-255.
[7] C. Guéneau, V. Dauvois, P. Pérodeaud, C. Gonella, O. Dugne, Liquid immiscibility in a (O,U,Zr) model corium. J. Nucl. Mater. 254 (1998) 158-174.
[8] P. Piluso, G. Trillon, C. Journeau, The UO_2-ZrO_2 system at high temperature (T > 2000 K) : importance of the metastable phases under severe accident conditions. J. Nucl. Mater. 344 (2005) 259–264.
[9] B. Sitaud, P.L. Solari, S. Schlutig, I. Llorens, H. Hermange, Characterization of radioactive materials using the MARS beamline at the synchrotron SOLEIL. J. Nucl. Mater. 425 (2012) 238-243.
[10] J.L. Hodeau, P. Bordet, M. Anne, A. Prat, A.N. Fitch, E. Dooryhee, G. Vaughan, A.K. Freund, Nine-crystal multi-analyser stage for high resolution powder diffraction between 6 and 40keV, Proc. SPIE 3448 (1998) 353-361.
[11] C. Dejoie, M. Coduri, S. Petitdemange, C. Giacobbe, E. Covacci, O. Grimaldi, P.O. Autran, M.W. Mogodi, D. S. Jung, A.N Fitch, Combining a nine-crystal multi-analyser stage with a two-dimensional detector for high-resolution powder X-ray diffraction. J. Appl. Cryst. 51 (2018) 1-13.
[12] A. Schökel, M. Etter, A. Berghäuser, A. Horst, D. Lindackers, Th.A. Whittle, S. Schmid, M. Acosta, M Knapp, H. Ehrenberg, M. Hinterstein, Multi-analyser detector (MAD) for high resolution and high energy powder x-ray diffraction. J. Synchr. Rad. 28 (2021) 146-157.
[13] A.H. Hill, T. Klimczuk, R. Springell, H.C. Walker, Measuring radioactive powder samples on the high-resolution powder diffraction beamline at the European Synchrotron Radiation Facility. J. Appl. Cryst. 46 (2013) 567–569.
[14] R. Guinebretiere, X-ray diffraction by polycrystalline materials, ISTE Ltd, London, 2007.
[15] K. Kakegawa, J. Mohri, T. Takahashi, H. Yamamura, S. Shirasaki, A compositional fluctuation and properties of $Pb(Zr,Ti)O_3$. Solid State Commun. 24 (1977) 769–772.
[16] K. Kakegawa, Y. Yoshino, H. Naruke, Y. Sasaki, Objective determination of the compositional fluctuation of $Pb(Zr, Ti)O_3$ and the effect of anisotropy in the sample on the determination. J. Mater. Sci. Lett. 16 (1997) 512–515.
[17] Y.-H. Han, M. Ishii, N. Uekawa, T. Kojima, K. Kakegawa, Preparation of homogeneous $Pb(Zr_xTi_{1-x})O_3$ by a rapid quenching technique and its compositional fluctuation. Scr. Mater. 56 (2007) 9–12.
[18] B.E. Warren "X-ray diffraction" Addison-Wesley, 1969.
[19] C.R. Houska, X-ray diffraction from a binary diffusion zone. J. Appl. Phys. 41 (1970) 69–75.
[20] D.R. Tenney, J.A. Carpenter, C.R. Houska, X-ray technique for the investigation of small diffusion zones. J. Appl. Phys. 41 (1970) 4485-4492.

[21] J. Unnam, C.R. Houska, An x-ray study of diffusion in the Cu-Ag system. J. Appl. Phys. 47 (1976) 4336–4342.

[22] C.R. Houska, Broadening of x-ray diffraction lines from small sub-grains containing gradients of spacing. J. Appl. Phys. 49 (1978) 2991–2993.

[23] C.R. Houska, X-ray examination of diffused films. Thin Solid Films 25 (1975) 451–464.

[24] B. Bolle, A. Tidu, J.J. Heizmann, X-ray diffraction study of concentration depth profiles of binary alloy coatings during thermal diffusion: application to brass coating. J. Appl. Cryst. 32 (1999) 27-35.

[25] D. Rafaja, M. Dopita, M. Masimov, V. Klemm, N. Wendt, W. Lengauer, Analysis of local composition gradients in the hard phase grains of cermets using a combination of X-ray diffraction and electron microscopy. Inter. J. Refrac. Met. Hard Mater. 26 (2008) 263-275.

[26] P. Buisson, P. Piluso, M. Pernet, M. Anne, Determination of the cationic composition distributions in mixed uranium and plutonium oxides by diffraction line profile analysis. Mater. Sci. Forum 378 (2001) 777-782.

[27] L. Lutterotti, Total pattern fitting for the combined size-strain-stress-texture determination in thin film diffraction. Nucl. Instrum. Methods Phys. Res. B 268 (2010) 334-340.

[28] J.I. Langford, The use of the Voigt function in determining microstructural properties from diffraction data by means of pattern decomposition. J. Appl. Cryst. 11 (1978) 10-14.

[29] G. Caglioti, A. Paoletti, F.P. Ricci, Choice of collimators for a crystal spectrometer for neutron diffraction. Nucl. Instrum. Methods Phys. 3 (1958) 223-228.

[30] D.J. Kim, Lattice parameters, ionic conductivities, and solubility limits in fluorite structure MO_2 oxide [M = Hf^{4+}, Zr^{4+}, Ce^{4+}, Th^{4+}, U^{4+}) solid solution. J. Am. Ceram. Soc. 72 (1989) 1415–1421.

[31] D. Fan, L.Q. Chen, Possibility of spinodal decomposition in ZrO_2-Y_2O_3 alloys: a theoretical investigation" J. Am. Ceram. Soc. 78 (995) 1680-1686.

[32] J. Katamura, N. Shibata, Y. Ikuhara, T. Sakuma, Transmission electron microscopy – energy dispersive X-ray spectroscopy analysis of the modulated structure in ZrO_2-6mol% Y_2O_3 alloy" Phil. Mag. Lett. 78 (1998) 45-49.

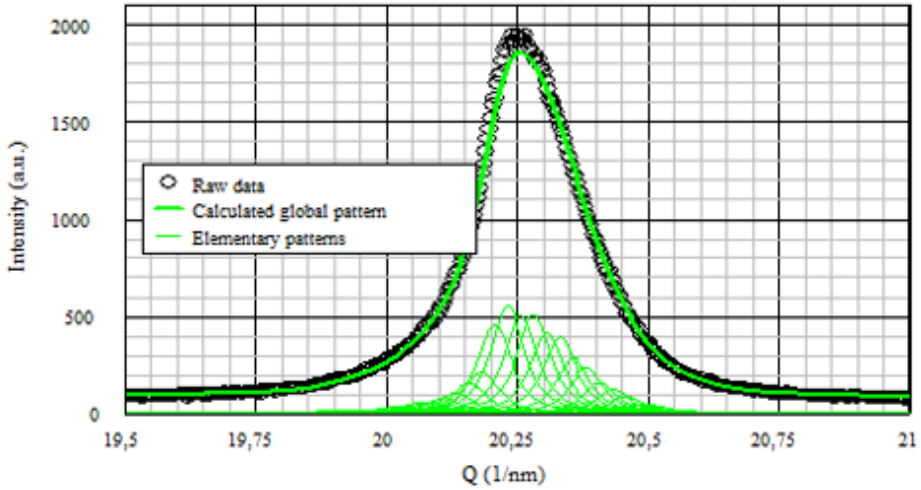
Intensity (a.u.)
2000
1500
1000
500
0
19,5
19,75
20
20,25
20,5
20,75
21
Q (1/nm)
Raw data
Calculated global pattern
Elementary patterns

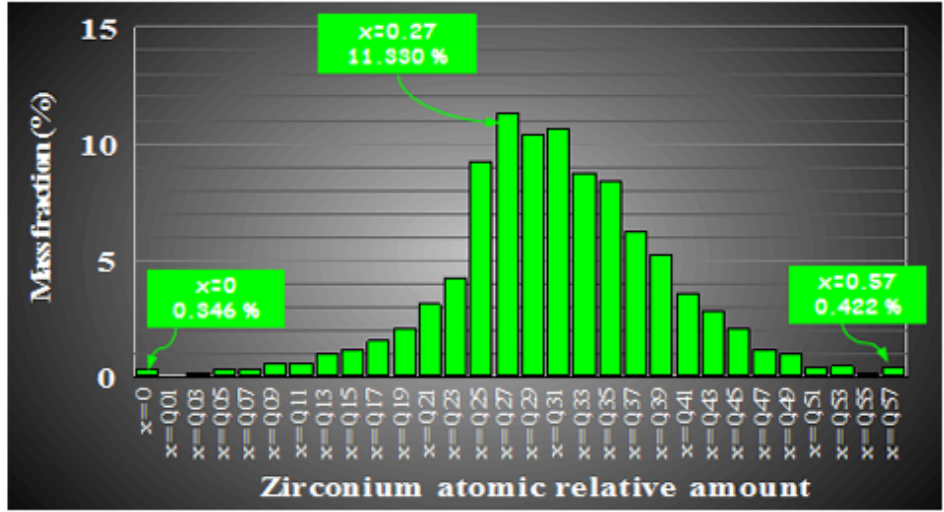
Mass fraction (%)
15
10
5
0
x=0.27
11.330 %
x=0
0.346 %
x=0.57
0.422 %
x=0
x=01
x=03
x=05
x=07
x=09
x=11
x=13
x=15
x=17
x=19
x=21
x=23
x=25
x=27
x=29
x=31
x=33
x=35
x=37
x=39
x=41
x=43
x=45
x=47
x=49
x=51
x=53
x=55
x=57
Zirconium atomic relative amount